



Contents lists available at ScienceDirect

Journal of Colloid and Interface Science

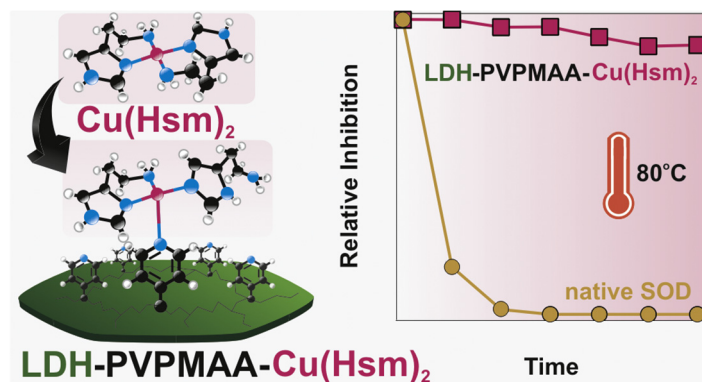
journal homepage: www.elsevier.com/locate/jcis

Regular Article

Highly stable enzyme-mimicking nanocomposite of antioxidant activity

Marko Pavlovic^a, Bálint Náfrádi^b, Paul Rouster^c, Szabolcs Muráth^{a,d}, Istvan Szilagyi^{a,d,*}^a MTA-SZTE Lendület Biocolloids Research Group, University of Szeged, H-6720 Szeged, Hungary^b Laboratory of Physics of Complex Matter, Ecole Polytechnique Fédérale de Lausanne, CH-1015 Lausanne, Switzerland^c Institute of Condensed Matter and Nanosciences – Bio and Soft Matter, Université Catholique de Louvain, B-1348 Louvain-la-Neuve, Belgium^d Interdisciplinary Excellence Center, Department of Physical Chemistry and Materials Science, University of Szeged, H-6720 Szeged, Hungary

GRAPHICAL ABSTRACT



ARTICLE INFO

Article history:

Received 31 January 2019

Revised 15 February 2019

Accepted 16 February 2019

Available online 16 February 2019

Keywords:

Antioxidant

Enzyme mimic

Nanoclay

Polymer functionalization

Dispersion stability

ABSTRACT

A highly stable nanocomposite of antioxidant activity was developed by immobilization of a superoxide dismutase-mimicking metal complex on copolymer-functionalized nanoclay. The layered double hydroxide (LDH) nanoclays were synthesized and surface modification was performed by adsorbing poly(vinylpyridine-*b*-methacrylic acid) (PVPMAA). The effect of the adsorption on the charging and aggregation properties was investigated and the copolymer dose was optimized to obtain stable LDH dispersions. The LDH-PVPMAA hybrid particles showed high resistance against salt-induced destabilization in aqueous dispersions. Copper(II)-histamine (Cu(Hsm)₂) complexes were immobilized via the formation of dative bonds between the metal ions and the nitrogen atoms of the functional groups of the copolymer adsorbed on the particles. Changes in the coordination geometry of the complex upon immobilization led to higher superoxide radical anion scavenging activity than the one determined for the non-immobilized complex. Comparison of superoxide dismutase (SOD)-like activity of the obtained hybrid LDH-PVPMAA-Cu(Hsm)₂ with the nanoclay-immobilized SOD enzyme revealed that the developed composite maintained its activity over several days and was able to function at elevated temperature, while the immobilized native enzyme lost its activity under these experimental conditions. The developed nanocomposite is a promising antioxidant candidate in applications, where high electrolyte concentration and elevated temperature are applied.

© 2019 Elsevier Inc. All rights reserved.

* Corresponding author at: MTA-SZTE Lendület Biocolloids Research Group, University of Szeged, H-6720 Szeged, Hungary.

E-mail address: szistvan@chem.u-szeged.hu (I. Szilagyi).

1. Introduction

Nanomaterials of enzyme-like features (so-called nanozymes) attracted considerable attention in the past decade to replace natural enzymes in order to overcome their high sensitivity to the environmental conditions such as pH, temperature and ionic strength [1]. In general, nanozymes consist of either bare nanoparticles or their functionalized derivatives [2]. In the first case, the materials themselves operate as a native enzyme, while in the latter case, metal complexes, which are able to mimic the structure and the function of natural metalloenzymes [3], are immobilized on nanoparticles to obtain enzyme-mimicking hybrid materials [4–6].

Nanozymes were also developed to replace antioxidant enzymes (e.g., superoxide dismutase (SOD), catalase (CAT), horseradish (HRP) and glutathione (GPx) peroxidases) [7], which are the primary defence systems against reactive oxygen species (ROS) such as superoxide, hydroxyl and peroxide radicals. Apart from their important roles in cell signalling [8], high ROS level leads to damage of biomolecules and causes various diseases including chronic inflammation and cancer [9]. Besides, the presence of ROS in formulation and chemical manufacturing processes in the food [10], pharmaceutical [11] and fuel [12] industry gives rise to lower quality products. The environmental conditions are especially harsh (e.g., elevated temperature or high ionic strength) in the industrial applications, therefore, antioxidant materials of high stability are required.

To develop efficient ROS scavenging systems, nanoparticles of various compositions were prepared. Among them, the most effective ones contained metal ions of redox activity, which mimic the function of the active centre of antioxidant enzymes and hence, they decompose ROS in redox reactions to molecular oxygen and/or water. For instance, Mn_3O_4 nanozyme was reported as a material with multi-enzymatic activity, since it was able to mimic the function of SOD, CAT and GPx enzymes and thus, it protected living cells against oxidative stress [13]. Biocompatible platinum nanoparticles were synthesized and showed effective scavenging activity for intracellular ROS [14]. Such a multi-enzymatic antioxidant function was also found for Prussian blue [15] and Co_3O_4 [16] nanoparticles, which were then applied as anti-inflammatory agent and in immunohistochemical assay, respectively. Bulk V_2O_5 was reported as toxic, however, V_2O_5 nanowires were found to be biocompatible and showed excellent GPx-mimicking properties [17].

Beside bare nanoparticle systems, composite nanomaterials were also reported as effective antioxidants. Self-assembly of V_2O_5 and MnO_2 nanoparticles through a dopamine linker led to high SOD, CAT and GPx-like activity and the obtained substance showed great promise in inflammation therapy [18]. The activity of some nanoparticle-based mimicking systems was even higher than the one determined for the native enzyme, like in the case of Pd-Ir core-shell HRP-mimicking nanoparticles [19]. It was shown that the peroxidase-like activity of nano-sized iron oxide can be tuned by surface functionalization due to the different affinity of the substrate to the coating molecules [20]. Appropriately chosen surface composition led to the development of a glucose sensor. In addition, triphenylphosphonium-conjugated ceria nanoparticles were prepared and used as antioxidant to reduce mitochondrial oxidative stress [21]. The role of the surface functional groups was to localize the mitochondria, while the ceria nanoparticles were responsible for the decomposition of ROS. Finally, SOD- and CAT-mimicking molecules were attached to cyclodextrin and the obtained hybrid compounds were processed into nanoparticle form, which significantly attenuated ROS-induced inflammation [22].

In the above examples, the antioxidant activity originated from the nanoparticles composed of metal ions with redox activity. In other systems, however, the nanoparticles were inactive in ROS scavenging and therefore, enzyme-mimetic activators were immobilized on their surface to achieve antioxidant activity. The most promising enzyme mimics contained transition metal ions [23,24] or their complexes [3,25,26] with structure similar to the one in the native enzymes. Such a structural mimic usually leads to a sufficient functional mimic too. The obtained nanoparticle-based hybrid composites were of similar ROS scavenging activity, but possessed a higher functional stability than the natural enzymes [27–29]. For instance, a copper(II)-zinc(II) heterobinuclear complex [30] of remarkable SOD activity [31] was immobilized on silica surface via either covalent bonds [32] or physical adsorption [33] and the obtained hybrid materials effectively mimicked the function of the native enzyme. Transition metal complexes of amino acids intercalated into clay materials [34] or covalently anchored to functionalized silica particles [35,36] were prepared and found to be efficient in dismutation of superoxide radical ions. Although the activity of these hybrids was lower than natural SOD, they exhibited the advantage of being less sensitive to the environmental conditions. In addition, hemin complexes were conjugated with montmorillonite [37] or to gold surfaces [38] to mimic peroxidase enzymes in oxidation reactions and hydrogen peroxide decomposition, respectively.

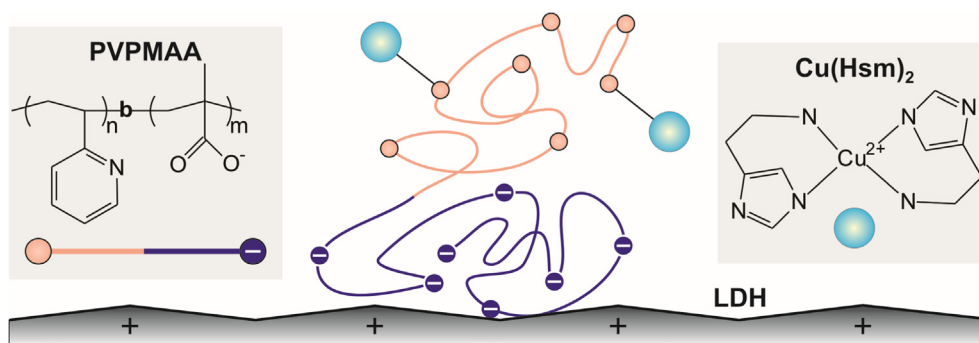
Apart from the enzymatic activity assessments and detailed structural characterization in solid state, these studies did not deal with the features of the obtained materials in dispersions. However, this is a critical point, since most of the applications took place in heterogeneous systems. Besides, there is a lack of information on the temperature-dependent functional stabilities, i.e., whether the antioxidant systems are able to act efficiently in ROS decomposition at higher temperatures or not. This issue is especially important in industrial applications of antioxidant materials, where elevated temperatures give rise to denaturation of the enzymes within short time intervals [39].

In the present work, SOD-mimicking nanozymes of high colloidal and functional stabilities were developed. Accordingly, copper(II)-histamine ($Cu(Hsm)_2$) complexes were immobilized on poly(vinylpyridine-*b*-methacrylic acid) (PVPMAA) copolymer-functionalized layered double hydroxide (LDH) nanoclay particles (Scheme 1). Thorough characterization of the obtained hybrid material (LDH-PVPMAA- $Cu(Hsm)_2$) was carried out in dispersions and the long-term functional stability as well as the temperature resistance in dismutation of superoxide radical anions were assessed.

2. Materials and methods

2.1. Chemicals

Chemicals including $Mg(NO_3)_2 \cdot 6H_2O$, $Al(NO_3)_3 \cdot 9H_2O$, NaOH, NaCl, NaH_2PO_4 , $CuCl_2$, nitro blue tetrazolium (NBT), histamine hydrochloride, xanthine oxidase (EC 1.17.3.2), xanthine, SOD (EC 1.15.1.1) were purchased from Sigma-Aldrich and used as received. The PVPMAA block copolymer was bought from Polymer Source and the number averaged molecular masses of the blocks were 10500 g/mol and 600 g/mol for PVP and MAA, respectively. For all experiments, ultrapure water produced by a Puranity TU3 UV/UF + water purification system (VWR) was used. Salt solutions and water applied in sample preparation for light scattering experiments were filtered with a syringe filter (Millex) of 0.1 μm pore size. The measurements were carried out at 25 °C and at pH (7.0 \pm 0.5).



Scheme 1. Illustration of the composition of the LDH-PVPMAA-Cu(Hsm)₂ hybrid material.

2.2. Preparation and functionalization of LDH

The nanoclay was prepared by the flash co-precipitation method [40]. In the synthesis, nitrate solutions of magnesium(II) and aluminium(III) metal ions were mixed in a 2:1 M ratio and the pH of the solution was increased to 9 by quickly adding appropriate amount of NaOH. The obtained precipitate was aged, filtered and dried prior to hydrothermal treatment at 120 °C. The resulting material was filtered and washed with water. The solid compound was then redispersed in water and used as stock dispersion in the sample preparation processes. The more detailed preparation of the LDH is given elsewhere [41].

In the colloid stability experiments, the LDH particles were modified with different amount of PVPMAA to follow the charging and aggregation processes in the dispersions. In these measurements, calculated amount of stock nanoclay dispersions and copolymer solutions were mixed at the desired ionic strength to keep the LDH dose at 10 mg/L and to vary the PVPMAA dose in the 1–1000 mg/g range. Note that the mg/g unit refers to mg copolymer per one gram of particle.

2.3. Characterization techniques

Electrophoretic mobilities were measured with a LiteSizer 500 (Anton Paar) device equipped with a 40 mW laser source operating at 658 nm wavelength. The experiments were performed in omega-shaped capillary cuvettes (Anton Paar). The average of five individual measurements was reported.

Hydrodynamic radii were determined by dynamic light scattering (DLS) using a NIBS/HPPS particle size analyzer (ALV GmbH). This instrument contains a He-Ne laser of 3 mW power and 633 nm wavelength. The measurements were carried out at 173° scattering angle in disposable plastic cuvettes (VWR) and the correlation function was collected for 20 s.

Powder X-ray diffraction experiments were performed on an Empyrean (PANalytical) diffractometer in the reflection geometry using the CuK α radiation (Johansson type Ge monochromator). The data were collected for 2-Theta ranging from 5° to 70° with a step of 0.0131 and for an exposure time of either 298 s or 798 s per step.

Infrared (IR) spectra were measured in the attenuated total reflectance (ATR) mode with a Spectrum 100 FT-IR spectrometer (PerkinElmer). The ATR crystal was made of diamond. The solid material was placed on the ATR crystal and the spectrum was recorded in the wavenumber range from 4000 to 400 cm⁻¹ at a resolution of 4 cm⁻¹. For the IR measurement, the solid materials were filtered from the dispersions, washed several times with water to remove weakly adsorbed copolymers and dried.

The electron paramagnetic resonance (EPR) spectroscopy measurements were carried out with a Bruker Elexsys E500 spectrometer operating at 9.4 GHz microwave frequency. The aqueous

solution used for the experiments was filled into 1.5 mm internal diameter Pyrex capillaries up to a height of 1 cm. The capillaries were arranged in a honeycomb structure inside a 4 mm outer diameter EPR capillary to minimize dielectric loss for an optimal signal-to-noise ratio. Care was taken to optimize the EPR accusation parameters to simultaneously obtain both broad and narrow spectral features without distortion. The analysis of the obtained spectra was performed with the EasySpin EPR spectrum simulation package [42].

Scanning electron microscopic (SEM) investigation was carried out using an S-4700 instrument (Hitachi) at various magnifications with 10 kV accelerating voltage. The sample was coated via physical noble metal vapour deposition to achieve electric conductivity.

The BET specific surface area was determined on the basis of N₂ adsorption-desorption isotherms with a NOVA 3000e device (Quantachrome Instruments).

2.4. Superoxide radical anion dismutation

The SOD-like activity was assessed in a standard biochemical assay [43]. Superoxide radical anions were produced by the reaction between xanthine and xanthine oxidase in the presence of NBT in phosphate buffer maintaining the pH at 7.5 during the reaction. Upon reduction by the radicals, NBT changes its colour from yellow to blue. The development of the absorption band at 565 nm was monitored with a Genesys 10S spectrophotometer (Thermo Scientific). The inhibition of the superoxide radical anion - NBT reaction by the scavenging compound was then calculated and the ability in dismutation of the superoxide radical anions was expressed in terms of IC₅₀ values, which correspond to the catalyst concentration necessary to decompose 50% of the radicals formed in the probe reaction. Moreover, long-term stability of the materials was measured and compared to the activity of the other catalysts (SOD, LDH-Hep-SOD (detailed characterization is given elsewhere [41]) and free Cu(Hsm)₂ complex). This was achieved by determining the IC₅₀ of the freshly prepared compounds and by comparing the initial 50% inhibition to the ones measured later. In that manner, the drop in the relative activity was followed during 4 days at room temperature or during 1 h at 80 °C.

The LDH-PVPMAA-Cu(Hsm)₂ material was prepared by mixing the nanoclay dispersion, the copolymer and the complex solutions at concentrations of 10 mg/L, 500 mg/g and 0.01 mM, respectively. The same samples were used in the EPR measurements. This condition was a compromise to obtain high colloidal and functional stability for the LDH-PVPMAA-Cu(Hsm)₂, as detailed later.

3. Results and discussion

A SOD-mimicking LDH-PVPMAA-Cu(Hsm)₂ material was prepared and investigated. LDH is a lamellar anionic clay [44], i.e., it

possesses anion exchange capacity, and is widely used as carrier in biomedical delivery processes due to the ease of synthesis, biocompatibility and tuneable size [45–50]. PVPMAA was chosen, because the negatively charged MAA groups are expected to adsorb on the oppositely charged LDH surface by electrostatic forces, while the pyridine groups of the PVP part contains nitrogen atoms, which may be able to bind to the copper(II) centre of the $\text{Cu}(\text{Hsm})_2$ complex through dative bonds leading to strong connection of the enzyme mimic to the copolymer-nanoclay carrier. The synthesis, characterization and SOD-like activity of the LDH-PVPMAA-Cu $(\text{Hsm})_2$ are detailed as follows.

3.1. Characterization of the nanoclay

The formation of the layered structure was confirmed by XRD and the diffraction pattern (Fig. S1a) contained all the characteristic reflections previously reported for LDH of similar composition [40,44,46]. The specific surface area of the nanoclay was determined to be $52.6 \text{ m}^2/\text{g}$ by the BET method. Morphologic analysis revealed that the material contains small grain-like platelets with rounded edges that form small aggregates in solid state. Such a hexagonal-based morphology is common among LDHs. The typical particle radius tends to be in the 50–100 nm range. DLS measurements yielded an average hydrodynamic radius of 110 nm and a polydispersity index of 0.3 in stable aqueous dispersions.

3.2. Adsorption of PVPMAA on LDH particles

The surface of the LDH particles was modified by adsorbing different amount of PVPMAA to tune its properties for further immobilization of the $\text{Cu}(\text{Hsm})_2$ complex. Note that the nanoclay is positively charged, while the PVPMAA is negatively charged under the experimental conditions applied. The adsorption process was followed by electrophoretic measurements, where the PVPMAA dose was systematically varied and the charging behaviour was investigated at different copolymer concentrations (Fig. 1).

The mobilities were positive at low copolymer concentration due to the positive structural charge of the bare particles [51], however, they decrease by increasing the dose clearly indicating that the adsorption of PVPMAA took place on the LDH. Such an adsorption led to charge neutralization at about 50 mg/g

copolymer dose. By further increasing the concentration, charge reversal was observed and the particles became negatively charged. Similar charge reversal has already been reported with LDH particles in the presence of oppositely charged polymers [41,52,53] or copolymers [54] and it originates from electrostatic attraction between the polymer and the surface, entropic gain due to the release of the solvent molecules [55] and hydrophobic interactions [56]. At high PVPMAA doses, the mobilities reached a plateau and remained constant within the experimental error. The value of about $-1.8 \times 10^{-8} \text{ m}^2/\text{Vs}$ corresponds to the electrophoretic mobility of the LDH-PVPMAA composite, which consists of the nanoclay and a self-assembled saturated copolymer surface layer at a dose of 500 mg/g.

The measurements were repeated at different ionic strengths (10 mM and 100 mM), however, the mobilities were very similar in the entire concentration range investigated (Fig. S2a). The doses needed for charge neutralization and surface saturation were significantly higher than the ones measured for pure poly(acrylic acid) (PAA) polyelectrolyte (Fig. S3a). This is due to the lower line charge density for the PVPMAA and thus, to the decreased repulsion between the negatively charged copolymer chains adsorbed on the surface.

Since the surface functionalized LDH will be used as carrier in dispersions, where highly stable primary particles are required, the colloidal stability was studied in the above systems. Accordingly, apparent aggregation rates (see Supporting Material (SM) for the details) were determined in the time-resolved DLS measurements. This technique has proven itself to be a powerful tool to investigate particle aggregation processes [51,57,58]. Thereafter, stability ratios [59] were calculated under the same experimental conditions as used in the above electrophoretic study (Fig. 1). Note that stability ratios close to unity correspond to rapidly aggregating samples and to unstable colloids, while higher values refer to more stable dispersions and to slower particle aggregation processes. In other words, the reciprocal of the stability ratios is equal to the fraction of particle collisions, which results in dimer formation. More details about the theoretical and practical backgrounds of the DLS measurements are given in the SM.

The measured U-shaped curve of the stability ratios at different copolymer doses resembles to the tendency reported for other systems containing LDH and oppositely charged polymers [51]. High stability ratios were obtained at low and high PVPMAA doses indicating stable dispersions. On the other hand, the samples were unstable in the intermediate concentration regime, where the stability ratios were one (deviations occurred only within the experimental error). Comparing the trends in the electrophoretic mobility and stability ratio data, one can realize that the unstable region is located at copolymer doses close to the charge neutralization point. The particles aggregate rapidly under these conditions and the aggregation process is controlled only by their diffusion.

The measurements were repeated at two more ionic strengths (Fig. S2b) to probe the effect of the salt concentration on the location of the slow and high aggregation regimes. No significant changes in the stability ratios were observed in the unstable region and at higher doses. However, the aggregation of the particles became rapid at low PVPMAA concentrations at 10 mM and 100 mM ionic strengths due to charge screening on the partially neutralized particles.

The stability ratio data measured at 1 mM ionic strength was compared to the ones determined with pure PAA (Fig. S3b). The unstable regime is located at lower polymer doses for PAA, since charge neutralization occurred at lower concentrations in that case. This fact also confirms that the fast aggregation regime is determined by the charge neutralization process of the particles.

The charging and aggregation behaviour of the particles at different PVPMAA doses are qualitatively in line with the theory

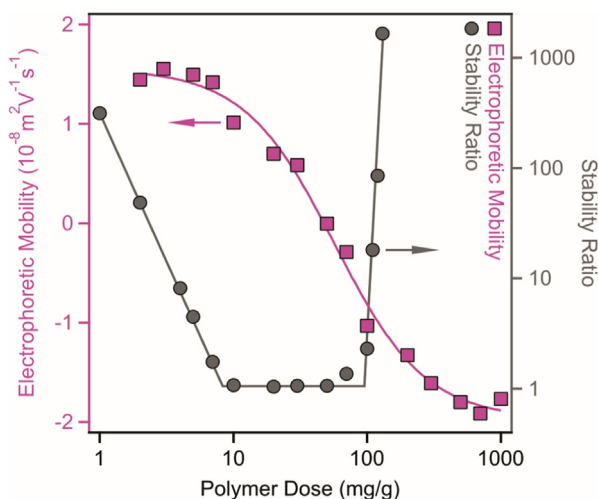


Fig. 1. Electrophoretic mobilities (squares) and stability ratios (circles) of the LDH particles in the presence of PVPMAA copolymer for different doses at 10 mg/L nanoclay concentration and 1 mM ionic strength adjusted by NaCl. The mg/g unit on the x-axis corresponds to mg of copolymer per one gram of LDH. The error in both mobility and stability ratio measurements is about 10%.

developed by Derjaguin, Landau, Verwey and Overbeek (DLVO) [60] to predict the colloidal stability of charged particles dispersed in electrolyte solutions. This theory states that such dispersions are stabilized by interparticle repulsions due to the presence of electrical double layers forming around the particles. At 1 mM ionic strength, this condition applies at low and high copolymer doses, where the functionalized LDH particles possess significantly high charges. However, attractive van der Waals forces are always present and the overall interparticle force is the sum of the attractive and repulsive forces. Once the charge of the particles is low or neutralized, the van der Waals forces overtake the repulsive ones and thus, the particles rapidly aggregate. In the dispersions containing LDH and PVPMAA, this condition applies at doses near the charge neutralization point.

The adsorption of the copolymer on the particles was also confirmed by IR spectroscopy by detecting the characteristic vibrations of both LDH and PVPMAA in the hybrid material. The spectra measured for the nanoclay particle, the copolymer and for its copolymer-functionalized derivative are shown in Fig. 2.

In the LDH-PVPMAA hybrid, a dose of 500 mg/g was applied, which corresponds to the PVPMAA concentration, where a saturated copolymer layer forms on the particle surface. Prior to the measurement, the LDH-PVPMAA material was filtered off, washed with water to remove the weakly adsorbed copolymer molecules and dried. The spectra clearly indicate that the adsorption process took place, since peaks originating from both LDH and PVPMAA could be detected in the spectrum of the composite material. Accordingly, 12 vibrational bands were observed for the LDH-PVPMAA, 6–6 corresponded to the carrier and the copolymer, respectively. For instance, the peaks at 447 cm^{-1} and at 781 cm^{-1} in the spectrum of LDH-PVPMAA are assigned to the Mg—O—H or

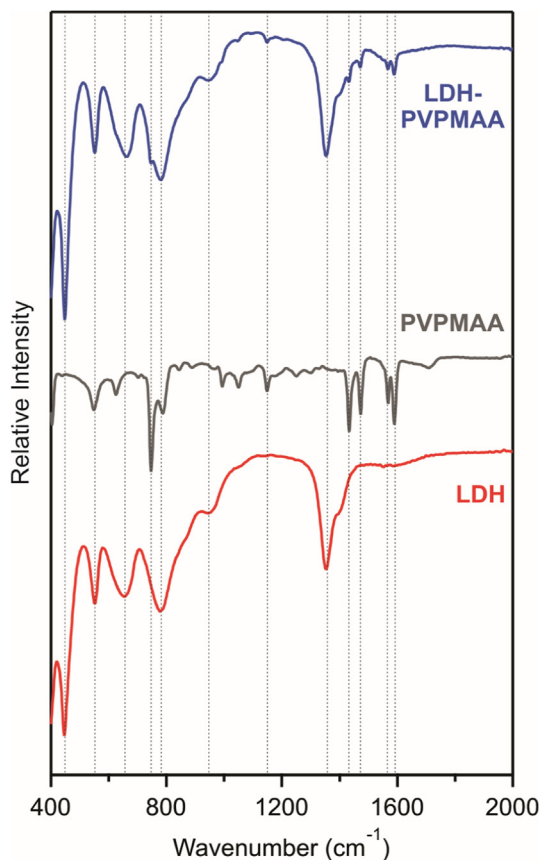


Fig. 2. IR spectra of the LDH, PVPMAA copolymer and the composite LDH-PVPMAA material. The latter one contains 500 mg of PVPMAA per one gram of LDH particle.

Al—O—H translations in the LDH [61]. The band at 1433 cm^{-1} originate from the wagging of the C—H bond in the pyridine group [62]. The ring stretching mode was observed at 1472 cm^{-1} confirming the successful adsorption of the PVPMAA on the LDH particles [63]. For the complete assignment of the IR peaks, see Table S1 in the SM.

3.3. Colloidal stability of the LDH-PVPMAA composite

The resistance of the LDH-PVPMAA material (LDH with a saturated copolymer surface layer) against salt-induced aggregation is an important issue in potential applications, where the nanocomposites are often dispersed in electrolyte solutions of high concentrations. Therefore, stability ratios of the hybrid were measured and compared to the ones determined for the bare particles to assess the stabilizing effect of the PVPMAA layer (Fig. 3).

Very similar dependencies were observed for the bare and copolymer coated LDH. Slow aggregation indicated by high stability ratios was observed at low ionic strengths, while the aggregation became rapid after a threshold salt concentration, which is the so-called critical coagulation concentration (CCC). Such a tendency of the stability ratios with varying salt level is predicted by the DLVO theory [60] and was reported for various charged colloidal particles dispersed in electrolyte solutions [51,64,65]. Repulsive forces generated by the electrical double layers weakened by increasing the ionic strength due to salt screening and they vanish at the CCC. Above this electrolyte concentration, attractive van der Waals forces predominate leading to rapid aggregation of the particles. Stability ratios close to unity above the CCC indicate diffusion controlled aggregation for both LDH and LDH-PVPMAA, which remained the same by further increasing the ionic strength.

Two observations in the tendencies deserve further discussion. First, the slope in the slow aggregation regime is smaller for the LDH-PVPMAA particles. This is due to surface heterogeneities upon copolymer functionalization. PVPMAA adsorbs non-uniformly on the surface and hence, forms islands (or patches) of negative charge [66]. These islands are electrostatically attracted to the empty surface places of another particle and thus, such a patch-charge attraction leads to additional attractive forces and to faster aggregation, i.e., lower stability ratios, and to smaller slopes in the

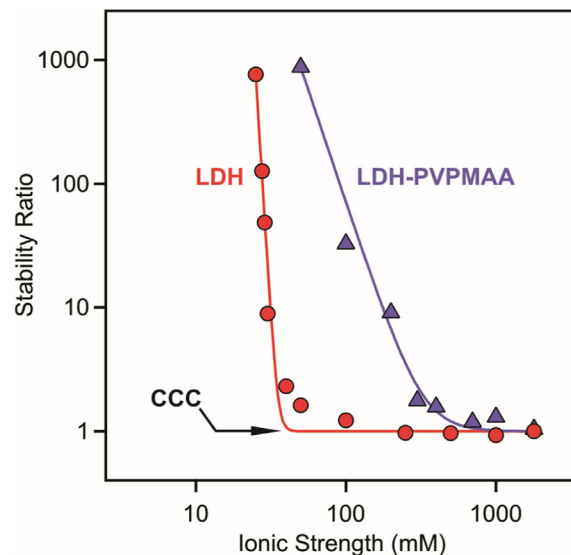


Fig. 3. Stability ratios of the LDH particles and LDH-PVPMAA composite material (500 mg of copolymer per gram of particles) as a function of the ionic strength adjusted by NaCl. The measurements were carried out at 10 mg/L particle concentration. The solid lines are fits obtained with equation S8.

slow aggregation regime [67]. The patch-charge interactions are absent in the case of the bare particles, since surface charge heterogeneities were formed upon the copolymer adsorption.

Second, the difference in the CCC values for LDH and LDH-PVPMAA is striking. A CCC of 40 mM was calculated for the bare and 610 mM for the copolymer coated particles. Such a large deviation in the CCC indicates the presence of strong repulsive forces. Electrophoretic mobility measurements carried out under the same experimental conditions (Fig. S4) revealed that the surface charge of the LDH and LDH-PVPMAA is comparable, therefore, the strong repulsive forces cannot originate only from the double layer repulsion in the latter case. Therefore, it was assumed that the particles are also stabilized by steric repulsion of the adsorbed copolymer chains. This type of interaction was found in several particle-polymer systems earlier [51,64,68,69]. The obtained high CCC for the LDH-PVPMAA indicates highly stable dispersions making the composite an excellent candidate for the further immobilization processes and for applications in samples of high ionic strength.

3.4. Immobilization of $\text{Cu}(\text{Hsm})_2$ on the LDH-PVPMAA particles

To mimic the function of the active centre of the SOD enzyme [70], $\text{Cu}(\text{Hsm})_2$ complex of 1:2 metal-to-ligand ratio was prepared by mixing the copper(II) salt with the histamine solution in 1:2 stoichiometric ratio at neutral pH. It was previously reported that the 4 nitrogen atoms of the ligand molecules are symmetrically coordinated to the metal ions forming an equatorial plane [71]. Accordingly, the donor atoms of the functional groups (pyridine nitrogen or carboxylic oxygen) in the LDH-PVPMAA hybrid material are expected to occupy one or two coordination places around the metal ion.

To follow the immobilization of the complex on the nanoclay-copolymer composite, electrophoretic mobilities and stability ratios were measured at different $\text{Cu}(\text{Hsm})_2$ concentrations (Fig. 4).

The tendencies in the mobilities and stability ratios were very similar to that observed for the LDH dispersions with systematic variation of the dose of the PVPMAA copolymer (Fig. 1). Obviously, the charge balance is opposite due to the negatively charged LDH-PVPMAA and $\text{Cu}(\text{Hsm})_2$ of positive charge. The mobilities increased by increasing the complex concentration indicating adsorption on the composite. The affinity of the coordination compound was high to the surface leading to charge neutralization and reversal at

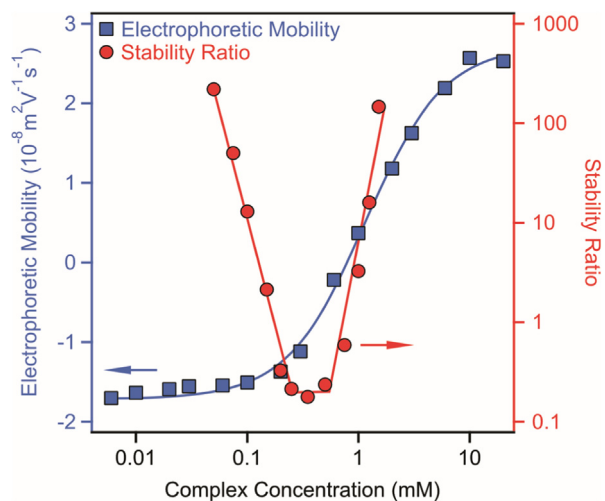


Fig. 4. Electrophoretic mobilities (squares) and stability ratios (circles) of the LDH-PVPMAA composite material as a function of the $\text{Cu}(\text{Hsm})_2$ complex concentration measured at 10 mg/L particle concentration.

appropriate concentrations. The corresponding stability ratios can be adequately explained by the charging behaviour and the DLVO theory. The intermediate region in the U-shape curve is located near the charge neutralization point, where van der Waals attractions are predominant in the absence of repulsive double layer forces. Besides, at low and high $\text{Cu}(\text{Hsm})_2$ concentrations, the dispersions are stable due to the presence of sufficiently charged particles and strong repulsive forces.

Although such a behaviour of charged colloidal particles in the presence of oppositely charged polyelectrolytes is common [51,64], it is rather atypical for divalent ions like the $\text{Cu}(\text{Hsm})_2$ complex. Charging and aggregation of LDH was investigated in salt solutions of various valences [51,72,73], however, such a high extent of charge inversions has not been reported yet. The restabilization of the dispersions by charge reversal is also a non-expected behaviour in this system. These results clearly indicate that a specific interaction takes place between the LDH-PVPMAA and the $\text{Cu}(\text{Hsm})_2$.

Given the structure of the copolymer, the formation of dative bonds between the copper(II) centre and the pyridine nitrogen or carboxylic oxygen of the adsorbed copolymer chain is feasible. To investigate the possibility of this scenario, EPR spectroscopy experiments were performed. This method is sensitive to the changes in the coordination geometry around metal ions of unpaired electrons like copper(II) [31,33,34], therefore, the spectra of the $\text{Cu}(\text{Hsm})_2$ in solution and on the LDH-PVPMAA surface were recorded (Fig. S5). A significant difference was found between the spectra indicating the different coordination geometry upon immobilization. The analysis of the measured spectrum for the LDH-PVPMAA- $\text{Cu}(\text{Hsm})_2$ material revealed that the EPR spectrum can be decomposed into two spectra of two independent copper(II) containing species (Fig. 5).

The fraction of the narrow component (A) is about 7% in both samples and it is unchanged upon immobilization on LDH-PVPMAA (Fig. S6) as confirmed by the same EPR parameters of $g_x = g_y = g_z = 2.12$ and $A = 210$ MHz. For species (A) the observed hyperfine interaction and the relatively narrow EPR linewidth indicate that the spin-spin interaction is weak and the species A are relatively rapidly moving.

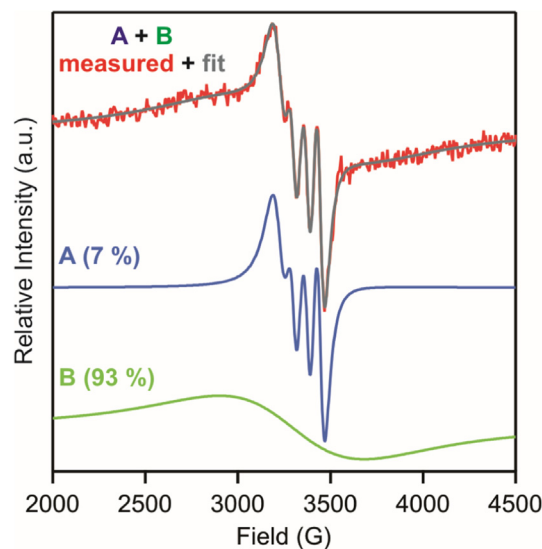


Fig. 5. Measured and fitted EPR spectra of the LDH-PVPMAA- $\text{Cu}(\text{Hsm})_2$ hybrid material (A + B, which contained about 7 mmol of $\text{Cu}(\text{Hsm})_2$ per one gram of LDH-PVPMAA) together with the calculated spectra of the two copper(II) containing components (A and B) existing in the sample. Note that the majority (93%) of the copper(II) centres are in component B.

The broad component (**B**) is 93% in both the free and immobilized complex and the structure is significantly different for the $\text{Cu}(\text{Hsm})_2$ in solution and on the surface. Spectrum analysis yielded $g_x = g_y = 2.05$ and $g_z = 2.25$ for the dissolved complex, while $g_x = g_y = g_z = 2.14$ once the $\text{Cu}(\text{Hsm})_2$ was attached to the LDH-PVPMAA. Hyperfine interaction was not resolved for the **B** species in neither configuration. These data shed light on that the coordination geometry around the metal centre in the **B** species is significantly different from the one in solution. Such a change in the arrangement of the donor atoms is most likely due to the coordination of the donor atoms of the functional groups of the LDH-PVPMAA composite to the metal centre of the complex.

Species with lower g_0 value show stronger ligand field in the equatorial plane, therefore, the coordination of 4 nitrogen atom is suggested for the dissolved complex. The higher g_0 value of the other isomer is probably produced by three equatorial nitrogen of the ligand and hence, one of the nitrogen of the $\text{Cu}(\text{Hsm})_2$ attached to the LDH-PVPMAA is forced to occupy the axial position. The coordination of carboxylic group oxygens of the copolymer may also occur in the fourth equatorial position, however, this cannot be unambiguously confirmed by the present EPR data. Nevertheless, the remarkable change in the coordination geometry with species **B** clearly indicate the complexation of the functional groups of the adsorbed PVPMAA by the copper(II) centre.

3.5. SOD-like activity of the LDH-PVPMAA- $\text{Cu}(\text{Hsm})_2$

The superoxide radical anion scavenging activity of the obtained LDH-PVPMAA- $\text{Cu}(\text{Hsm})_2$ was probed in a biochemical test reaction [43] and compared to the activity of the non-immobilized $\text{Cu}(\text{Hsm})_2$, SOD and LDH-immobilized SOD enzyme (LDH-Hep-SOD) reported earlier [41]. In addition, the long-term stability and the temperature resistance of the SOD-like function were tested.

In the assay, the inhibition of the reaction between the NBT indicator compound and superoxide radical anions formed in situ was measured as a function of the copper(II) content of the enzyme or the mimicking complex (Fig. S7). The activities of the materials were expressed in terms of IC_{50} values, which is equal to the copper(II) concentration necessary to dismutate 50% of the radicals forming in the test reaction. These values were found to be $2.6 \times 10^{-1} \mu\text{M}$, $9.7 \times 10^{-2} \mu\text{M}$, $2.1 \times 10^{-3} \mu\text{M}$ and $2.9 \times 10^{-3} \mu\text{M}$ for $\text{Cu}(\text{Hsm})_2$, LDH-PVPMAA- $\text{Cu}(\text{Hsm})_2$, SOD and LDH-Hep-SOD, respectively.

Although the IC_{50} determined for the native and immobilized enzymes were lower, the $\text{Cu}(\text{Hsm})_2$ still showed significant SOD-like function. Besides, the activity of the complex increased upon immobilization, since a lower IC_{50} was measured for the LDH-PVPMAA- $\text{Cu}(\text{Hsm})_2$ compared to $\text{Cu}(\text{Hsm})_2$. Such an improved activity is due to the changes in the coordination geometry around the copper(II) ions (see the results of the EPR measurements in the previous chapter) once the donor atoms from the adsorbed copolymer is coordinated giving rise to an evolved structure allowing a more efficient scavenging of the superoxide radical anions. The IC_{50} of the LDH-PVPMAA- $\text{Cu}(\text{Hsm})_2$ is greater than those previously reported for SOD-mimicking metal complexes [30,31,34,74] and for the immobilized ones [32–34,75].

To probe the long-term stability of the hybrid material, the IC_{50} values were measured over 4 days for the above compounds and the relative activities, i.e., the data were normalized to the IC_{50} determined with the freshly prepared samples, were calculated. Fig. 6 shows the obtained tendencies in the long-term activities.

Although the native SOD kept its functional integrity, the immobilized derivative lost about 80% of its activity during the time period investigated. Such a decrease occurred most probably due to slow conformational changes on the surface, which led to a

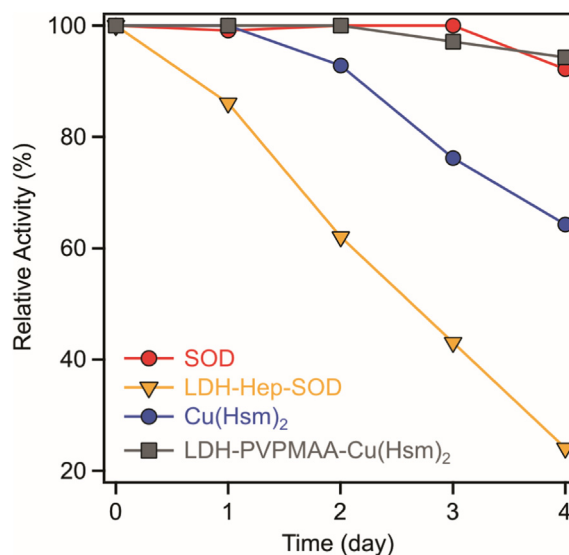


Fig. 6. Relative superoxide radical anion scavenging activity (related to the freshly prepared samples) of the native SOD (red circle), its immobilized form (LDH-Hep-SOD, yellow triangle), the $\text{Cu}(\text{Hsm})_2$ complex (blue circle) and the LDH-PVPMAA- $\text{Cu}(\text{Hsm})_2$ (grey square) hybrid material over 4 days measured at room temperature. Note that the error of the measurements is about 15%. (For interpretation of the references to colour in this figure legend, the reader is referred to the web version of this article.)

loss of the superoxide radical anion dismutation ability. Comparing the $\text{Cu}(\text{Hsm})_2$ and LDH-PVPMAA- $\text{Cu}(\text{Hsm})_2$, the relative activity of the complex in solution decreased significantly, however, the immobilized complex was of about the same efficiency after 4 days. This behaviour was similar to the one experienced by the native enzyme. Accordingly, the attachment of the $\text{Cu}(\text{Hsm})_2$ to the copolymer-functionalized LDH gave rise to the formation of a hybrid material of high functional stability.

In the next step, the temperature resistance of the SOD-like function was investigated. The IC_{50} values were determined at 80°C periodically after 10 min for 1 h. The relative activities were again calculated as the obtained IC_{50} data normalized to the one

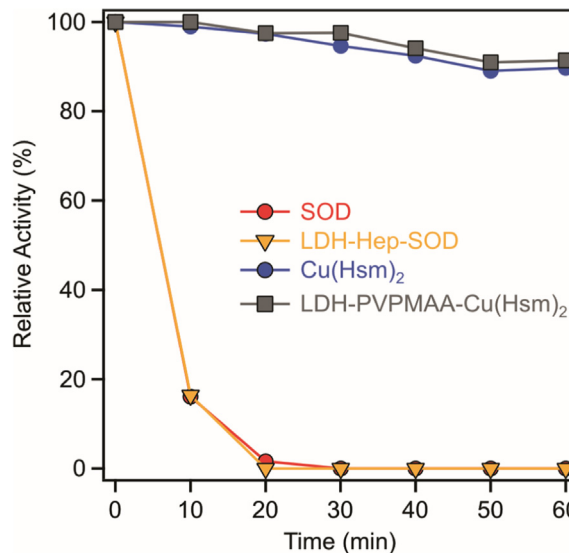


Fig. 7. Relative superoxide radical anion dismutating activities of the native SOD (red circle), its immobilized form (LDH-Hep-SOD, yellow triangle), the $\text{Cu}(\text{Hsm})_2$ complex (blue circle) and the LDH-PVPMAA- $\text{Cu}(\text{Hsm})_2$ (grey square) composite over 1 h at 80°C . (For interpretation of the references to colour in this figure legend, the reader is referred to the web version of this article.)

measured immediately after sample preparation and equilibration at 80 °C (Fig. 7).

Both native and immobilized SOD quickly lost their activities and denatured after about 20 min, while the Cu(Hsm)₂ and LDH-PVPMAA-Cu(Hsm)₂ kept 90% of their initial superoxide radical anion scavenging ability after 1 h. These results shed light on the fact that replacing the natural enzyme with the mimicking compounds led to the development of an antioxidant material of significant SOD-like activity even at elevated temperature.

Combining the results presented in Figs. 6 and 7, the following conclusions were taken. First, immobilization of the copper(II) complex significantly improved its long-term activity and the obtained LDH-PVPMAA-Cu(Hsm)₂ behaves in a similar manner as the native SOD. Second, the enzyme is not able to function at higher temperature, while the enzyme-mimicking composite is still highly active. In addition, the LDH-PVPMAA-Cu(Hsm)₂ forms highly stable colloid and the catalytic centres are linked with strong primary chemical bonds to the surface of the carrier particles. Accordingly, the obtained nanoclay-copolymer-complex hybrid material is an extremely promising candidate in applications, wherever longer term antioxidant effects are required in dispersions of high electrolyte concentrations or at elevated temperature.

4. Conclusions

Antioxidant hybrid nanomaterial (LDH-PVPMAA-Cu(Hsm)₂) composed of nanoclay carrier, copolymer stabilizer and copper(II) complex as catalytic centre was prepared, characterized and tested in dismutation of superoxide radical anions. The experimental conditions for the functionalization of the LDH with PVPMAA were optimized in order to obtain LDH-PVPMAA composite of high colloidal stability. The Cu(Hsm)₂ was successfully immobilized through dative bonds formed between the donor atoms of the adsorbed copolymer chains and the metal centre of the complex.

Structural changes in the coordination geometry around the copper(II) ions upon immobilization led to higher functional stability in dismutation of superoxide radical anions in comparison to the one determined for the complex in solution. The LDH-PVPMAA-Cu(Hsm)₂ kept its radical scavenging function for longer time period compared to the free Cu(Hsm)₂ and immobilized SOD. Moreover, the hybrid nanomaterial was highly active even at 80 °C, a condition, where the native or immobilized SOD enzyme quickly lost their antioxidant activity.

The obtained material is able to solve problems connected to ROS damage in the textile, food and cosmetic industry, where the manufacturing processes often take place in dispersions of high electrolyte concentration and/or at elevated temperature. Such an antioxidant effect is beneficial to produce good quality products of long term stability. Therefore, the LDH-PVPMAA-Cu(Hsm)₂ nanohybrid can be recommended as an efficient antioxidant.

Acknowledgements

The financial support by the Lendület program of the Hungarian Academy of Sciences (96130) and by the Ministry of Human Capacities, Hungary through grant 20391-3/2018/FEKUSTRAT is gratefully acknowledged. This work was also partially supported by the Swiss National Science Foundation (200021_144419). The authors thank Professors Michal Borkovec and László Forró for the possibility to use the facilities in their laboratories.

Appendix A. Supplementary material

Supplementary data to this article can be found online at <https://doi.org/10.1016/j.jcis.2019.02.050>.

References

- [1] H. Wei, E.K. Wang, *Chem. Soc. Rev.* 42 (2013) 6060–6093.
- [2] Y.H. Lin, J.S. Ren, X.G. Qu, *Adv. Mater.* 26 (2014) 4200–4217.
- [3] R. Breslow, *Chem. Rec.* 1 (2001) 3–11.
- [4] G.Y. Tonga, Y.D. Jeong, B. Duncan, T. Mizuhara, R. Mout, R. Das, S.T. Kim, Y.C. Yeh, B. Yan, S. Hou, V.M. Rotello, *Nat. Chem.* 7 (2015) 597–603.
- [5] K. Kirkorian, A. Ellis, L.J. Twyman, *Chem. Soc. Rev.* 41 (2012) 6138–6159.
- [6] O. Kudina, A. Zakharchenko, O. Trotsenko, A. Tokarev, L. Ionov, G. Stoychev, N. Pureskiy, S.W. Pryor, A. Voronov, S. Minko, *Angew. Chem.-Int. Edit.* 53 (2014) 483–487.
- [7] M.A. El-Missiry, *Antioxidant Enzyme*, InTech, Rijeka, 2012.
- [8] B. D'Autreaux, M.B. Toledano, *Nat. Rev. Mol. Cell Biol.* 8 (2007) 813–824.
- [9] S. Reuter, S.C. Gupta, M.M. Chaturvedi, B.B. Aggarwal, *Free Radic. Biol. Med.* 49 (2010) 1603–1616.
- [10] J.W. Finley, A.N. Kong, K.J. Hintze, E.H. Jeffery, L.L. Ji, X.G. Lei, *J. Agric. Food Chem.* 59 (2011) 6837–6846.
- [11] C. Nirmala, M.S. Bisht, H.K. Bajwa, O. Santosh, *Trends Food Sci. Technol.* 77 (2018) 91–99.
- [12] D.F. Grishin, *Pet. Chem.* 57 (2017) 813–825.
- [13] N. Singh, M.A. Savanur, S. Srivastava, P. D'Silva, G. Mugesh, *Angew. Chem.-Int. Edit.* 56 (2017) 14267–14271.
- [14] M. Moglianetti, E. De Luca, P.A. Deborah, R. Marotta, T. Catelani, B. Sartori, H. Amenitsch, S.F. Retta, P.P. Pompa, *Nanoscale* 8 (2016) 3739–3752.
- [15] W. Zhang, S.L. Hu, J.J. Yin, W.W. He, W. Lu, M. Ma, N. Gu, Y. Zhang, *J. Am. Chem. Soc.* 138 (2016) 5860–5865.
- [16] J.L. Dong, L.N. Song, J.J. Yin, W.W. He, Y.H. Wu, N. Gu, Y. Zhang, *A.C.S. Appl. Mater. Interf.* 6 (2014) 1959–1970.
- [17] A.A. Vernekar, D. Sinha, S. Srivastava, P.U. Paramasivam, P. D'Silva, G. Mugesh, *Nat. Commun.* 5 (2014).
- [18] Y.Y. Huang, Z. Liu, C.Q. Liu, E.G. Ju, Y. Zhang, J.S. Ren, X.G. Qu, *Angew. Chem.-Int. Edit.* 55 (2016) 6646–6650.
- [19] X.H. Xia, J.T. Zhang, N. Lu, M.J. Kim, K. Ghale, Y. Xu, E. McKenzie, J.B. Liu, H.H. Yet, *ACS Nano* 9 (2015) 9994–10004.
- [20] F.Q. Yu, Y.Z. Huang, A.J. Cole, V.C. Yang, *Biomaterials* 30 (2009) 4716–4722.
- [21] H.J. Kwon, M.Y. Cha, D. Kim, D.K. Kim, M. Soh, K. Shin, T. Hyeon, I. Mook-Jung, *ACS Nano* 10 (2016) 2860–2870.
- [22] Y.Q. Wang, L.L. Li, W.B. Zhao, Y. Dou, H.J. An, H. Tao, X.Q. Xu, Y. Jia, S. Lu, J.X. Zhang, H.Y. Hu, *ACS Nano* 12 (2018) 8943–8960.
- [23] M. Vazquez-Gonzalez, W.C. Liao, R. Gazelles, S. Wang, X. Yu, V. Gutkin, I. Willner, *ACS Nano* 11 (2017) 3247–3253.
- [24] A. Pratsinis, G.A. Kelesidis, S. Zuercher, F. Krumeich, S. Bolisetty, R. Mezzenga, J. C. Leroux, G.A. Sotiriou, *ACS Nano* 11 (2017) 12210–12218.
- [25] C. Belle, J.L. Pierre, *Eur. J. Inorg. Chem.* (2003) 4137–4146.
- [26] A.J. Wu, J.E. Penner-Hahn, V.L. Pecoraro, *Chem. Rev.* 104 (2004) 903–938.
- [27] B. Sels, D. De Vos, M. Buntinx, F. Pierard, A. Kirsch-De Mesmaeker, P. Jacobs, *Nature* 400 (1999) 855–857.
- [28] P. Vanelderden, J. Vancauwenbergh, B.F. Sels, R.A. Schoonheydt, *Coord. Chem. Rev.* 257 (2013) 483–494.
- [29] M.R. Maurya, A. Kumar, J.C. Pessoa, *Coord. Chem. Rev.* 255 (2011) 2315–2344.
- [30] H. Ohtsu, Y. Shimazaki, A. Odani, O. Yamauchi, W. Mori, S. Itoh, S. Fukuzumi, *J. Am. Chem. Soc.* 122 (2000) 5733–5741.
- [31] I. Szilagy, I. Labadi, K. Hernadi, I. Palinko, N.V. Nagy, L. Korecz, A. Rockenbauer, Z. Kele, T. Kiss, *J. Inorg. Biochem.* 99 (2005) 1619–1629.
- [32] Y.C. Fang, H.C. Lin, I.J. Hsu, T.S. Lin, C.Y. Mou, *J. Phys. Chem. C* 115 (2011) 20639–20652.
- [33] I. Szilagy, I. Labadi, K. Hernadi, I. Palinko, I. Fekete, L. Korecz, A. Rockenbauer, T. Kiss, *New J. Chem.* 29 (2005) 740–745.
- [34] I. Szilagy, I. Labadi, K. Hernadi, T. Kiss, I. Palinko, *Molecular Sieves: From Basic Research to Industrial Applications*, Pts a and b, 2005, pp. 1011–1018.
- [35] Z. Csendes, C. Dudas, G. Varga, E.G. Bajnóczi, S.E. Canton, P. Sipos, I. Palinko, *J. Mol. Struct.* 1044 (2013) 39–45.
- [36] M. Yang, W. Jiang, Z.Q. Pan, H. Zhou, *J. Inorg. Organomet. Polym. Mater.* 25 (2015) 1289–1297.
- [37] L.H. Zhang, C. Gu, J. Xiong, M. Yang, Y. Guo, *Sci. China-Chem.* 58 (2015) 731–737.
- [38] K. Sengupta, S. Chatterjee, A. Dey, *ACS Catal.* 6 (2016) 1382–1388.
- [39] R.M. Daniel, M. Dines, H.H. Petach, *Biochem. J.* 317 (1996) 1–11.
- [40] Z.P. Xu, G.S. Stevenson, C.Q. Lu, G.Q.M. Lu, P.F. Bartlett, P.P. Gray, *J. Am. Chem. Soc.* 128 (2006) 36–37.
- [41] M. Pavlovic, P. Rouster, I. Szilagy, *Nanoscale* 9 (2017) 369–379.
- [42] S. Stoll, A. Schweiger, *J. Magn. Reson.* 178 (2006) 42–55.
- [43] C. Beaucham, I. Fridovich, *Anal. Biochem.* 44 (1971) 276–287.
- [44] Q. Wang, D. O'Hare, *Chem. Rev.* 112 (2012) 4124–4155.
- [45] G. Choi, H. Piao, M.H. Kim, J.H. Choy, *Ind. Eng. Chem. Res.* 55 (2016) 11211–11224.
- [46] C. Forano, F. Bruna, C. Mousty, V. Prevot, *Chem. Rec.* 18 (2018) 1150–1166.
- [47] Z. Gu, J.J. Atherton, Z.P. Xu, *Chem. Commun.* 51 (2015) 3024–3036.
- [48] S. Vial, V. Prevot, F. Leroux, C. Forano, *Micropor. Mesopor. Mat.* 107 (2008) 190–201.
- [49] V.J. Nagaraj, X. Sun, J. Mehta, M. Martin, T. Ngo, S.K. Dey, *J. Nanotech.* 2015 (2015) 350370.
- [50] N.K. Singh, Q.V. Nguyen, B.S. Kim, D.S. Lee, *Nanoscale* 7 (2015) 3043–3054.
- [51] M. Pavlovic, P. Rouster, T. Oncsik, I. Szilagy, *ChemPlusChem* 82 (2017) 121–131.

- [52] C. Vasti, A. Borgiallo, C.E. Giacomelli, R. Rojas, *Coll. Surf. A* 533 (2017) 316–322.
- [53] V. Hornok, A. Erdohelyi, I. Dekany, *Coll. Polym. Sci.* 283 (2005) 1050–1055.
- [54] M. Pavlovic, M. Adok-Sipiczki, C. Nardin, S. Pearson, E. Bourgeat-Lami, V. Prevot, I. Szilagy, *Langmuir* 31 (2015) 12609–12617.
- [55] S.Y. Park, R.F. Bruinsma, W.M. Gelbart, *Europhys. Lett.* 46 (1999) 454–460.
- [56] J.Y. Carrillo, A.V. Dobrynin, *Langmuir* 23 (2007) 2472–2482.
- [57] J.A. Smith, O. Werzer, G.B. Webber, G.G. Warr, R. Atkin, *J. Phys. Chem. Lett.* 1 (2010) 64–68.
- [58] M. Kobayashi, M. Skarba, P. Galletto, D. Cakara, M. Borkovec, *J. Coll. Interf. Sci.* 292 (2005) 139–147.
- [59] M. Elimelech, J. Gregory, X. Jia, R.A. Williams, *Particle Deposition and Aggregation: Measurement, Modeling, and Simulation*, Butterworth-Heinemann Ltd., Oxford, 1995.
- [60] D.F. Evans, H. Wennerstrom, *The Colloidal Domain*, John Wiley, New York, 1999.
- [61] J.H. Lee, S.W. Rhee, D.Y. Jung, *Bull. Korean Chem. Soc.* 26 (2005) 248–252.
- [62] C.Y. Wang, M.H. Cui, *J. Appl. Polym. Sci.* 88 (2003) 1632–1636.
- [63] B.L. Li, X.L. Lu, Y.H. Ma, Z. Chen, *Eur. Polym. J.* 60 (2014) 255–261.
- [64] S. Muráth, S. Sáringer, Z. Somosi, I. Szilagy, *Coll. Interf.* 2 (2018) 32.
- [65] C. Schneider, M. Hanisch, B. Wedel, A. Jusufi, M. Ballauff, *J. Coll. Interf. Sci.* 358 (2011) 62–67.
- [66] I. Popa, G. Papastavrou, M. Borkovec, *Phys. Chem. Chem. Phys.* 12 (2010) 4863–4871.
- [67] Y.K. Leong, *Coll. Polym. Sci.* 277 (1999) 299–305.
- [68] E. Illes, E. Tombacz, *J. Coll. Interf. Sci.* 295 (2006) 115–123.
- [69] A. Tiraferri, L.A.S. Hernandez, C. Bianco, T. Tosco, R. Sethi, *J. Nanopart. Res.* 19 (2017).
- [70] J.S. Richardson, K.A. Thomas, B.H. Rubin, D.C. Richardson, *Proc. Natl. Acad. Sci. USA.* 72 (1975) 1349–1353.
- [71] C.G. Zhang, C.Y. Duan, Q. Hu, D.Y. Yan, *J. Chem. Crystallogr.* 29 (1999) 1153–1155.
- [72] G. Lagaly, O. Mecking, D. Penner, *Coll. Polym. Sci.* 279 (2001) 1090–1096.
- [73] M. Pavlovic, R. Huber, M. Adok-Sipiczki, C. Nardin, I. Szilagy, *Soft Matter* 12 (2016) 4024–4033.
- [74] W.S. Terra, S.S. Ferreira, R.O. Costa, L.L. Mendes, R.W.A. Franco, A.J. Bortoluzzi, J. Resende, C. Fernandes, A. Horn, *Inorg. Chim. Acta* 450 (2016) 353–363.
- [75] M. Mureseanu, M. Puscasu, S. Somacescu, G. Carja, *Catal. Lett.* 145 (2015) 1529–1540.